Multiple phases with intertwined magnetic and superconducting orders in Nd-doped CeCoIn_{5}

Duk Y. Kim, Shi-Zeng Lin, Franziska Weickert, P. F. S. Rosa, Eric D. Bauer, Filip Ronning, J. D. Thompson, and Roman Movshovich

Multiple phases with intertwined magnetic and superconducting orders in Nd-doped CeCoIn$_5$

Duk Y. Kim,[*] Shi-Zeng Lin, Franziska Weickert, P. F. S. Rosa, Eric
D. Bauer, Filip Ronning, J. D. Thompson, and Roman Movshovich[†]

Los Alamos National Laboratory, Los Alamos, New Mexico 87545, USA

The thermal conductivity of heavy-fermion superconductor Ce$_{0.95}$Nd$_{0.05}$CoIn$_5$ was measured with a magnetic field rotating in the tetragonal *a-b* plane. The thermal conductivity exhibits a step within the high-field low-temperature (HFLT) phase, which exists above 8 Tesla within the superconducting state, when field is rotated through the antinodal [100] direction of the superconducting *d*-wave order parameter. This anomaly indicates the presence of a third order parameter within the HFLT phase, similar to that of pure CeCoIn$_5$. Therefore, the HFLT state with triply intertwined orders, i.e., superconducting *d*-wave, magnetic spin-density wave (SDW), and a putative superconducting *p*-wave pair-density wave (PDW), is robust against 5% Nd doping. The second magnetic phase within the superconducting state below 8 Tesla, a low-field SDW, displays a hysteresis in thermal conductivity as a function of field magnitude, which is also revealing the existence of a third order consistent with a *p*-wave PDW. Given different origins and properties of the HFLT and low-field SDW states, the presence of three intertwined orders in both phases is remarkable and of far-reaching consequences.

I. INTRODUCTION

Magnetic and superconducting phase transitions are by far the most frequent examples of electronic ordering in condensed matter. When electrons are strongly correlated, complex and not well-understood relationships between ordered states are possible. Instead of competing, a common view of the interaction between magnetic and superconducting orders, these states can stabilize one another at a microscopic level. CeCoIn$_5$ is an ultimate example of such interaction, where magnetic order, present in a high field and low temperature (HFLT) of the superconducting phase[1], disappears together with superconductivity at a superconducting critical field[2,3]. Magnetism in CeCoIn$_5$, therefore, needs superconductivity for its very existence, presenting a clear-cut example of two orders that are intimately intertwined[4]. Recent thermal conductivity measurements revealed the simultaneous formation of a third intertwined order in HFLT phase, which was putatively identified as a *p*-wave pair-density wave (PDW)[5].

Ce$_{0.95}$Nd$_{0.05}$CoIn$_5$ presents a more complicated phase diagram, where two phases with SDW order were identified within its superconducting state via neutron scattering measurements, as shown in the inset of Fig. 1(a). Both form with the same ordering wavevector $\mathbf{Q}$ = (0.44, ±0.44, 0.5) as that in the HFLT phase of pure CeCoIn$_5$, where $\mathbf{Q}$ is pinned along nodes of the *d*-wave superconducting gap[6–8]. Though not proven definitively, the two SDW orders may have different origins: the SDW in the HFLT phase arises from field-induced condensation of magnetic excitations in a zero-field spin resonance that is present in both pure and Nd-doped CeCoIn$_5$[9–11], while the SDW at low fields results from cooperative effects between impurity-induced islands of antiferromagnetism[12]. Another theoretical study shows that magnetic impurities can induce the SDW order also by condensing magnetic excitations[13]. Regardless of the origin of the low-field SDW state, both the high-field and the low-field SDW states are suppressed to T = 0 in the vicinity of 8 T[6].

These observations raise fundamental questions, including what is the nature of the two potentially distinct phases and their interrelation; whether a PDW, or more specifically a *p*-

wave PDW, exists in either the high- or low-field phases; and, with seemingly identical symmetries of both the SDW and superconducting orders at low and high field, whether there is a field-induced quantum critical point between the two phases and what might drive it. Here, we report thermal conductivity measurements on Nd-doped CeCoIn$_5$ in both its low- and high-field SDW states, with magnetic field rotating within the *a-b* plane of this tetragonal compound. These experiments demonstrate that a third order (presumably *p*-wave PDW) is present in both SDW phases of Ce$_{0.95}$Nd$_{0.05}$CoIn$_5$, indicating the ubiquitous nature of such order in the presence of magnetic SDW and *d*-wave superconducting orders.

II. METHODS

CeCoIn$_5$ single crystals with 5% Nd were grown from an excess indium flux. The crystal structure and the actual Nd concentration were confirmed by x-ray diffraction and energy-dispersive x-ray analysis, respectively. Thermal conductivity measurements were performed similarly to those on undoped CeCoIn$_5$ reported elsewhere[5]. The crystal of Ce$_{0.95}$Nd$_{0.05}$CoIn$_5$ was polished into a thin rectangular plate ($2.8 \times 0.4 \times 0.1\ mm^3$) with the longest edge along the [110] direction. Heat current was applied along the [110] direction and the crystal was rotated about its *c* axis with a piezoelectric rotator in the presence of a magnetic field applied within the *a-b* plane.

III. RESULTS

A number of properties of the superconducting state in Ce$_{0.95}$Nd$_{0.05}$CoIn$_5$ are similar to those of pure CeCoIn$_5$. Figure 1(a) shows the temperature dependence of the thermal conductivity of Ce$_{0.95}$Nd$_{0.05}$CoIn$_5$, with the heat current along the nodal direction of the *d*-wave order parameter, and the field directed just off the anti-nodal direction. At zero magnetic field, κ/T at 2.5 K is approximately half of the value for undoped CeCoIn$_5$[5], reasonably due to increased scattering by
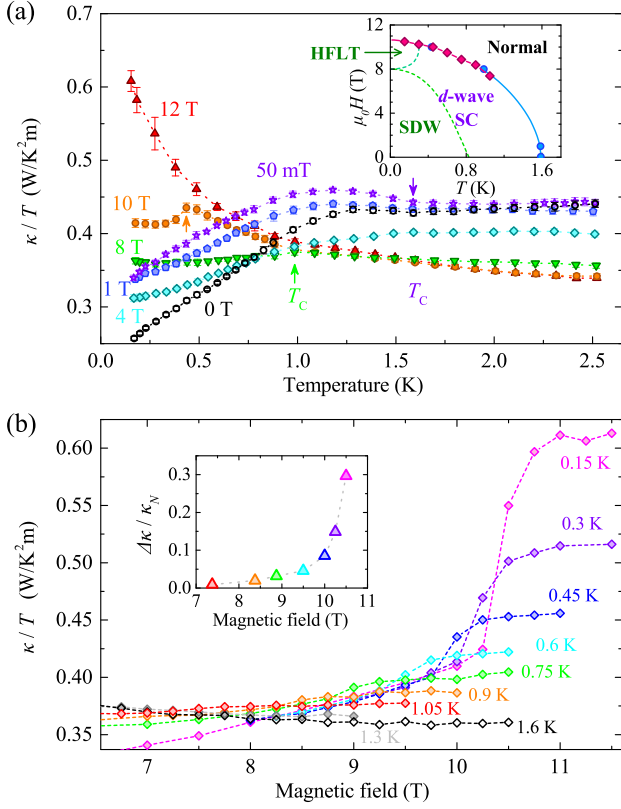
FIG. 1. (a) The thermal conductivity κ of 5% Nd-doped CeCoIn$_5$ divided by temperature T as a function of temperature in several magnetic fields. Arrows depict the onsets of the superconducting transition. Inset: Schematic phase diagram of 5% Nd-doped CeCoIn$_5$[6]. Superconducting–normal transition points are acquired in the present study. Red diamonds are from field sweeps and blue dots are from temperature sweeps. (b) κ/T as a function of field for several temperatures. All scans are performed with decreasing magnetic field. The evolution of κ/T near H_{c2} demonstrates the first-order nature of the superconducting transition at low temperature. Inset: The change in thermal conductivity $\Delta\kappa$ from just below to just above H_{c2} divided by the thermal conductivity in the normal state κ_N just above H_{c2}. The direction of the magnetic field for both (a) and (b) is 5° away from the [100] direction in the a-b plane ($\theta = 40°$).

impurities, and comparable to that of CeCoIn$_5$ doped with a similar concentration of non-magnetic La[14]. An increase (a kink) of the thermal conductivity below 1.6 K at fields below 1 T indicates an increase in electron mean-free path due to the onset of superconductivity. A downward kink at T_c develops at fields above 8 T, and a sharp drop in the curve at 10 T reflects the first-order nature of the superconducting transition, in accord with neutron-scattering experiments[6]. At 12 T, which is above the upper critical field H_{c2}, κ/T increases with decreasing temperature, characteristic of the non-Fermi-liquid behavior observed in pure CeCoIn$_5$[15].

Figure 1(b) plots the evolution of the high-field superconducting transition anomaly in κ/T vs. field H with temperature. As temperature increases, the thermal-conductivity jump at H_{c2}, characteristic of the first-order nature of the superconducting transition, decreases and disappears entirely above 1.3
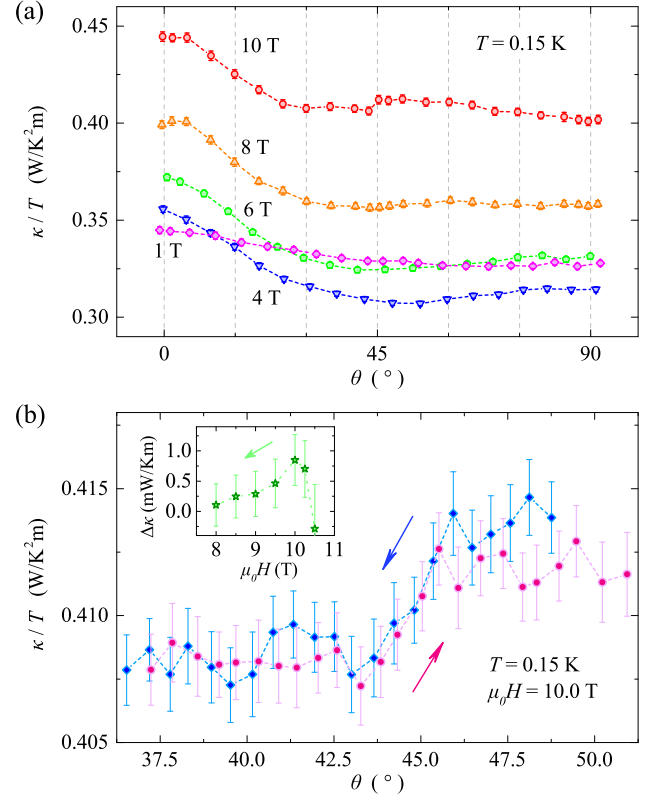
FIG. 2. The dependence of the thermal conductivity divided by temperature (κ/T) on the angle θ between the applied field $\mathbf{H}$ and the heat current $\mathbf{J}$ that is along [110]. (a) κ/T at 0.15 K for several values of field, in both phases with SDW order. Additional data for wider angles are presented in Fig. 5 (Appendix B). (b) Thermal conductivity jumps when a magnetic field of 10 T is rotated though the [100] ($\theta = 45°$) direction. Inset: The difference between the thermal conductivities of field-down scans at $\theta = 40°$ and $\theta = 50°$.

K. The first-order superconducting transitions are indicated by red diamonds in the inset of Fig. 1(a), consistent with neutron-scattering measurements[6]. The inset of Fig. 1(b) shows that the magnitude of the discontinuous jump of thermal conductivity at the transition increases with field. This behavior, characteristic of undoped CeCoIn$_5$[16], is due to strong Pauli limiting, an important ingredient in a number of theoretical proposals for the nature of the HFLT state in CeCoIn$_5$. The persistence of the first-order transition in 5% Nd-doped CeCoIn$_5$ is in stark contrast with previous doping studies in which a tiny amount of doping by Cd, Hg, or Sn on In sites (less than 0.1%) broadened the specific heat anomaly associated with the superconducting transition in high fields, reflecting the suppression of its first-order character[17,18]. Our studies demonstrate that the first-order superconducting transition in CeCoIn$_5$ is much more robust to introduction of Nd impurities on the Ce site.

Measurements in a rotating magnetic field have proven to be a powerful probe of superconducting states. This is particularly true for CeCoIn$_5$, where the d-wave symmetry of the superconducting order was identified via thermal conductivity[19], and detailed properties of the HFLT state were studied by both

neutron-scattering[20] and thermal-conductivity measurements[5] in rotating field. In Fig. 2, we display the thermal conductivity of $Ce_{0.95}Nd_{0.05}CoIn_5$ as a function of the angle θ between the heat current $\mathbf{J} \parallel$ [110] direction and the rotating magnetic field. Data for the full 90° scan at 0.15 K are shown for several fields in Fig. 2(a). In the HFLT phase, a small step at 45° was observed. As shown by the fine-step scan at 10 T in the main panel of Fig. 2(b), thermal conductivity jumps sharply when magnetic field is rotated through the [100] anti-nodal direction for the $d_{x^2-y^2}$ superconducting order parameter ($\theta = 45°$, see insets in Fig. 3). Similar behavior is observed in undoped $CeCoIn_5$[5] where the anomaly is narrower and greater in size, both by roughly an order of magnitude. It reflects switching of the ordering wave vector $\mathbf{Q}$ of the single-domain SDW[20]. Recent neutron-scattering measurements in rotating magnetic field in $Ce_{0.95}Nd_{0.05}CoIn_5$ also showed switching of the SDW ordering wave vector between the two nodal directions in the HFLT phase[21], with $\mathbf{Q}$ aligning with the node most perpendicular to the magnetic field. The switching occurs within the angle of the field rotation similar to our thermal conductivity results. Therefore, when the field is closer to the [110] direction of the heat current $\mathbf{J}$ ($\theta < 45°$), $\mathbf{Q}$ is along (0.44, -0.44, 0.5), which is perpendicular to $\mathbf{J}$. The measured thermal conductivity in this case is lower than that with the field further away from the heat current direction ($\theta > 45°$, $\mathbf{Q} =$ (0.44, 0.44, 0.5)). This behavior is opposite to that expected from the effect of the SDW alone, which gaps states along $\mathbf{Q}$, and, therefore, reduces the thermal conductivity when $\mathbf{Q}$ is along the nodal direction same as $\mathbf{J}$. The field dependence of thermal conductivity in the HFLT phase, similarly to the case of pure $CeCoIn_5$[5], therefore, indicates the existence of an additional superconducting order parameter (consistent with a p-wave pair-density wave (PDW)) that gaps quasiparticles along the nodal direction perpendicular to the $\mathbf{Q}$ of the SDW.

In contrast to results in the HFLT state of $Ce_{0.95}Nd_{0.05}CoIn_5$, there is no detectable step in thermal conductivity during field rotation in the low-field ($\mu_0 H < 8$ T) SDW phase, in particular around $\mathbf{H} \parallel$ [100] ($\theta = 45°$) where it appears in the HFLT phase, and, therefore, no indication of single-domain switching behavior. In addition to data in Fig. 2(a), fine-step measurements around $\theta = 45°$ with 1 and 6 T magnetic field show no sharp step, as displayed in Fig. 4 (Appendix A). The absence of step below 8 T could be due to several effects, including a multi-domain nature of the low-field SDW phase and strong pinning by the Nd impurities. The field-sweep thermal-conductivity measurements described below show hysteresis in evidence of a multi-domain structure of the SDW phase.

Figure 3 displays the thermal conductivity of $Ce_{0.95}Nd_{0.05}CoIn_5$ as a function of magnetic field for several directions of field with respect to the heat current. For these measurements, magnetic field was swept from zero to 12 T and then decreased back to zero. The data show hysteresis, which argues immediately for multiple inequivalent domains in the SDW phase.

Neutron-scattering experiments on 5% Nd-doped $CeCoIn_5$ demonstrated convincingly that the magnetic ordering wave vectors in the HFLT and low-field SDW phases are identical[6].
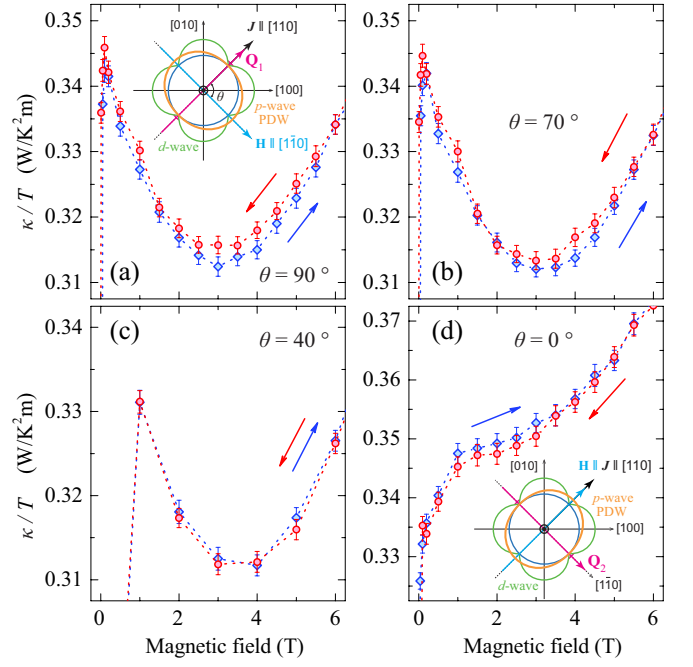

FIG. 3. The thermal conductivity divided by temperature (κ/T) at 0.15 K measured while sweeping field from 0 to 12 T and then back to 0 T for four different field directions. Hysteresis is observed around 4 T in all but one ($\theta = 40°$) directions. No hysteresis is observed above 6 T within the experimental uncertainty. Insets: Diagrams of the experimental setup and the intertwined orders. Blue circle – schematic Fermi surface; Green – $d_{x^2-y^2}$ superconducting order parameter; Pink arrow – SDW ordering wave vector $\mathbf{Q}$; Orange – p-wave PDW superconducting order parameter; Cyan arrow – applied magnetic field $\mathbf{H}$; Black arrow – heat current $\mathbf{J}$; θ is the angle between the heat current and the magnetic field. Both $\mathbf{Q}$ and the p-wave order flip 90° when the field is switched between two perpendicular nodal directions in (a) and (d).

Nd impurities reduce the magnetic coherence length of the SDW, and at zero field (with no preferred direction imposed by the magnetic field) the SDW state forms in a multi-domain structure with equal population of $\mathbf{Q}_1 = (0.44, 0.44, 0.5)$ and $\mathbf{Q}_2 = (0.44, -0.44, 0.5)$ domains[21]. Increasing magnitude of the field gradually aligns the $\mathbf{Q}$'s of the domains to lie perpendicular to the field direction, and hysteresis of thermal conductivity in field sweeps are consistent with these results. Though there is no evidence for hypersensitive switching of $\mathbf{Q}$ in the low-field SDW phase, spin-orbit coupling between SDW order and an applied field, which is a proposed mechanism for this sensitivity in the single-domain structure of the HFLT state of $CeCoIn_5$, also can account for the observed hysteresis[22]. Spin-orbit coupling, which favors selection of a particular $\mathbf{Q}$ most perpendicular to magnetic field, is also present in $Ce_{0.95}Nd_{0.05}CoIn_5$ and, with increasing field $\mathbf{H} \parallel$ [1$\bar{1}$0], would tend to switch $\mathbf{Q}_2$ domains into $\mathbf{Q}_1$ domains[21]. Such switching should be hysteretic when the SDW experiences some pinning due to impurities. Impurity pinning is also the origin of a broadened switching anomaly in the HFLT phase shown in Fig. 2(b).

Features of the data displayed in Fig. 3 are consistent with

this scenario. Hysteresis is most pronounced in field-swept curves for $\theta = 90°$ and $0°$ (see Figs. 3(a) and 3(d)). This is expected, as magnetic field is most effective in switching ordering vectors $\mathbf{Q}$ that are originally parallel to $\mathbf{H}$ to be aligned perpendicular to $\mathbf{H}$[22]. The field at $\theta = 0°$ flips $\mathbf{Q}_1$ into $\mathbf{Q}_2$ domains, and the field at $\theta = 90°$ does the opposite, flipping $\mathbf{Q}_2$ domains into $\mathbf{Q}_1$. Within this picture, the field at $\theta = 70°$ is less effective at aligning domains, with correspondingly smaller hysteresis compared to $\theta = 90°$. Progressively, the field close to [100], $\theta = 40°$, should be even less efficient at flipping domains, reducing hysteresis even further. This is precisely what the data show in Figs. 3(b) and 3(c), respectively, as hysteresis at $70°$ is less than that at $90°$, and no hysteresis is observed at all at $40°$.

Figures 3(a) and 3(d) show that the thermal conductivity on increasing field is lower when $\theta = 90°$ but higher when $\theta = 0°$. As the field aligns the domains ordering wave vectors $\mathbf{Q}$ perpendicular to the field direction on the field-up sweep, the domains' $\mathbf{Q}$ remain preferentially aligned that way on the field-down sweep, $\mathbf{Q}_1$ for $\theta = 90°$ (Fig. 3a) and $\mathbf{Q}_2$ for $\theta = 0°$ (Fig. 3d). The signs of the difference (hysteresis) for both field orientations show that domains with $\mathbf{Q}_1$ have greater thermal conductivity than the domains with $\mathbf{Q}_2$, exactly the same behavior as in the HFLT phases of pure and Nd-doped CeCoIn$_5$. Therefore, just as in the case of the HFLT phase, an additional order is required, which reduces thermal conductivity along a direction perpendicular to $\mathbf{Q}$. The p-wave PDW that gaps electronic states along the nodes perpendicular to $\mathbf{Q}$, expected in a d-wave superconductor with an SDW order[23], would explain the thermal conductivity data in the low-field SDW phase just as it does in the HFLT phase. The sharp jump of thermal conductivity observed in the HFLT phase, displayed in Fig. 2(b), is approximately 1% of the thermal conductivity. The magnitude of the hysteresis in the LF-SDW phase is also approximately 1% of the thermal conductivity (see in Fig. 3(a,d)). This suggests that the amplitudes of the order parameters of the p-wave PDW are similar in both phases.

IV. DISCUSSION

The existence of a putative superconducting p-wave PDW orders in both HFLT and low-field SDW states is striking, considering that these states are different in several crucial aspects. **I**. The low-field SDW phase is induced by magnetic Nd impurities, but the HFLT state forms without or with Nd impurities. Further, the zero-field spin fluctuations in Ce$_{0.95}$Nd$_{0.05}$CoIn$_5$ appear to be unaffected by the development of SDW order; whereas formation of magnetic order in the HFLT phase is tied intimately to excitations in the spin resonance[11]. **II**. An applied field has the opposite effect on these phases: magnetic field suppresses the low-field SDW phase but stabilizes the HFLT phase in both Ce$_{0.95}$Nd$_{0.05}$CoIn$_5$ and pure CeCoIn$_5$. Suppression of the low-field SDW by an applied in-plane magnetic field is understood to be due to field-induced tilting of Nd moments from out-of-plane to in-plane direction, which weakens the magnetization

of impurity-induced droplets of local SDW correlations and, consequently, the temperature at which the long-range SDW order develops[24]. In contrast, a field-split excitation mode of the spin resonance softens and approaches zero for fields where the HFLT phase develops[9]. **III**. The mechanism driving the hypersensitivity to the field angle in the HFLT phase (in pure and Nd-doped compounds) is either absent or not strong enough to overcome SDW pinning by impurities that induce the low-field SDW phase of Ce$_{0.95}$Nd$_{0.05}$CoIn$_5$. There is, however, a gradual field-induced reorientation of domains within the low-field SDW phase[21]. As discussed, this reorientation may be due to the spin-orbit interaction[22] that could account for the hypersensitivity in pure CeCoIn$_5$. Field-induced tipping of Nd moments toward the a-b plane may weaken impurity pinning of SDW domains, which would restore hypersensitivity in the HFLT phase. Alternatively, the HFLT phase may be realization of a spatially inhomogeneous Fulde-Ferrel-Larkin-Ochinnikov (FFLO) superconducting state[25,26], a scenario originally suggested for pure CeCoIn$_5$[2]. Recently, the FFLO order has been proposed to be the main cause of the hypersensitivity in its HFLT state[27,28]. In contrast, an FFLO state will not form at zero and low fields in the SDW phase.

In summary, in-plane field-angle thermal-conductivity measurements on Ce$_{0.95}$Nd$_{0.05}$CoIn$_5$ reveal signatures of a third order, likely to be p-wave PDW, in its low-field SDW and HFLT phases and show that the HFLT phase of CeCoIn$_5$ and its intertwined orders are robust against 5% Nd doping. Given different origins and properties of the low-field SDW and the HFLT states, the presence of a p-wave PDW in both phases emphasizes that it is ubiquitous in the company of coupled superconducting d-wave and magnetic SDW orders, suggesting the general nature of this phenomenon. Strongly correlated electron superconductors on the verge of magnetic order, such as copper-oxide, organic, iron-based and other heavy-fermion materials, would be likely candidates to exhibit similar intertwined orders. Imaging the spatial dependence of the superconducting condensate, via e.g. scanning tunneling spectroscopy, would be very useful in elucidating the nature of the intertwined states in such systems.
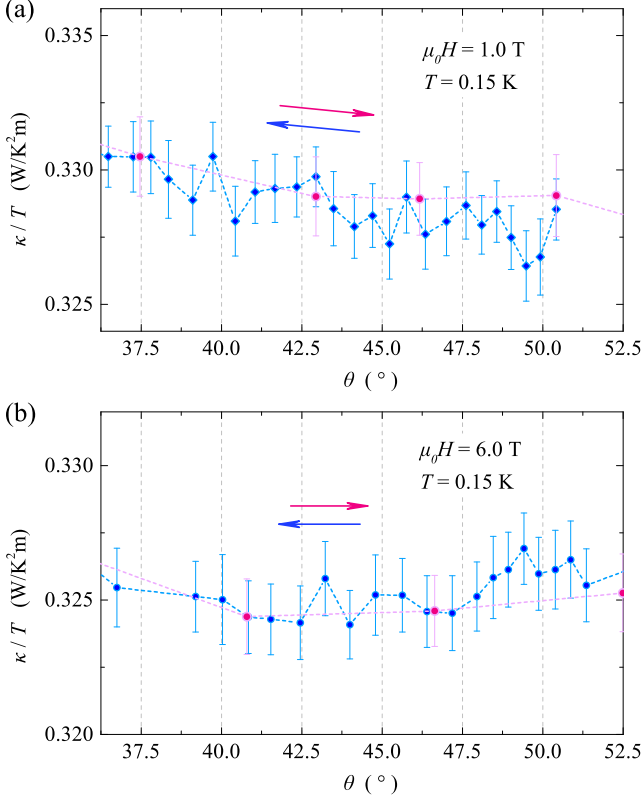
(a)

(b)

FIG. 4. The field-angle dependence of κ/T near **H** ∥ [100] with 1-T (a) and 6-T (b) magnetic field.

Appendix A: Absence of hypersensitive switching in the low-field SDW phase

Thermal conductivity was carefully measured when the magnetic field was rotated though the [100] ($\theta = 45°$) direction. Figure 4 shows the results of the fine-rotation measurments with the magnetic field of 1 T and 6 T. With the magnetic field lower than 8 T, no sharp jump of thermal conductivity around $\theta = 45°$ was observed.

Appendix B: 180° rotation of the magnetic field

In order to show the periodicity, the thermal conductivity with a 180° field rotation is plotted in Fig. 5. The increased thermal conductivity when the field is along the heat current direction ($\theta = 0°$) can be understood with the increasing mean-free path of nodal quasiparticles[29].

Appendix C: The effect of impurities on the HFLT phase

Although the properties of HFLT phases in pure and Nd-doped CeCoIn$_5$ are qualitatively the same, there are detailed differences. The relative magnitude of the jump in thermal conductivity in the high-field phase of the Nd-doped sample
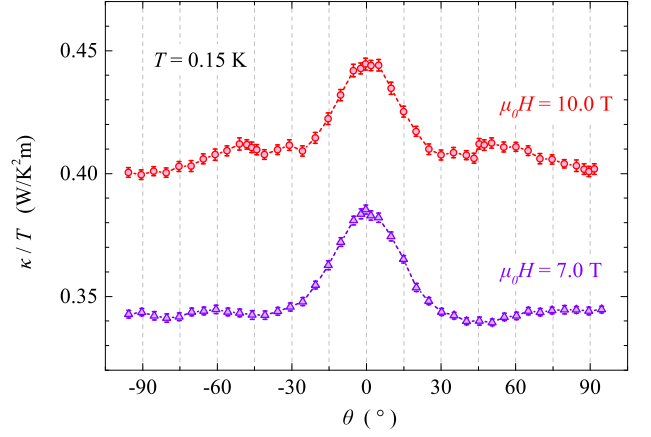

FIG. 5. The field-angle dependence of κ/T between $\theta = -90°$ and $\theta = 90°$

is approximately 1%, an order of magnitude smaller than approximately 15% found in pure CeCoIn$_5$. This reduction is likely due to magnetic pair breaking by Nd impurities creating normal quasiparticles that partially fill the d-wave nodes and reducing the influence of both SDW and PDW on thermal transport. Secondly, the width of the transitions region (step) in thermal conductivity of Ce$_{0.95}$Nd$_{0.05}$CoIn$_5$ upon field rotation is $\Delta\theta = 3 \sim 10°$, an order of magnitude larger than that in CeCoIn$_5$ at a similar temperature[5,20]. Broadening of the transition is consistent with the range of pinning interactions within the transition region due to randomness in Ce-site occupancies by Nd impurities[30]. Overall, however, both the HFLT state and the first-order nature of the superconducting transition at low temperature appear to be much more robust to the introduction of impurities on the Ce site than on the In sites of CeCoIn$_5$.

Appendix D: Thermal codncutivity jump with a tiny magnetic field

Figure 6 shows the thermal coudncutivty as a function of field from zero to above H_{c2}. The sharp increase of thermal conductivity from its zero-field value brought on by the tiny magnetic field of 50 mT is similar to that in pure CeCoIn$_5$, which was attributed to a multi-band nature of superconductivity in CeCoIn$_5$, with a very small superconducting energy gap in a band of light electrons[31]. This observation of the multi-band superconductivity suggests that 5% Nd doping does not change the band structure of CeCoIn$_5$ significantly.

Appendix E: On single- vs. double-Q structure of the SDW order

For the low-field SDW phase, it has been shown theoretically that dilute magnetic impurities can induce SDW order in a d-wave superconductor with underlying magnetic
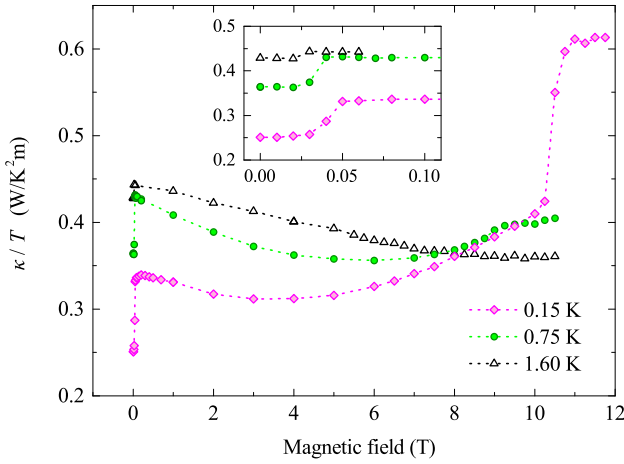
FIG. 6. The magnetic-field dependence of κ/T. The inset shows an expanded view of the data near zero field, which are collected with increasing field from zero-field-cooled states. The data above 1 T are the same as those in Fig. 1(b). The direction of the magnetic field is 5° away from the [100] direction in the a-b plane.

correlations[12]. The local density of states enhanced by impurities can induce patches of static local oscillation of magnetization around impurities, and the cooperative Ruderman-Kittel-Kasuya-Yosida (RKKY) exchange effect between impurities can generate long-range SDW order[12,32]. Another theory shows that the magnetic impurities induce the SDW order by condensing excitations in the spin resonance[13]. According to these models, impurities facilitate the development of SDW order without an applied magnetic field. In this zero-field phase, the four-fold symmetry of the d-wave superconducting order should be present. The SDW should appear with ordering wave vectors along the two perpendicular nodal directions with equal ordered moments in each domains[24], and result in equal neutron-scattering intensities at these two $\mathbf{Q}$'s. Our experiment on $Ce_{0.95}Nd_{0.05}CoIn_5$ shows that if the order in SDW phase were double-$\mathbf{Q}$, the coupling between external rotating magnetic field and such a double-$\mathbf{Q}$ state would be smooth and continuous, without a sharp-step characteristic of the single-$\mathbf{Q}$ HFLT phase. However, the observed hysteresis would necessitate the presence of p-wave PDW in such state as well. The nature, strength, and consequences of the interaction between the impurity-induced SDW and the magnetic field remain open questions.

* dukyng@gmail.com
† roman@lanl.gov

[1] M. Kenzelmann, Reports on Progress in Physics **80**, 34501 (2017).
[2] A. Bianchi, R. Movshovich, C. Capan, P. G. Pagliuso, and J. L. Sarrao, Phys. Rev. Lett. **91**, 187004 (2003).
[3] M. Kenzelmann, S. Gerber, N. Egetenmeyer, J. L. Gavilano, T. Strässle, A. D. Bianchi, E. Ressouche, R. Movshovich, E. D. Bauer, J. L. Sarrao, and J. D. Thompson, Phys. Rev. Lett. **104**, 127001 (2010).
[4] E. Fradkin, S. A. Kivelson, and J. M. Tranquada, Rev. Mod. Phys. **87**, 457 (2015).
[5] D. Y. Kim, S.-Z. Lin, F. Weickert, M. Kenzelmann, E. D. Bauer, F. Ronning, J. D. Thompson, and R. Movshovich, Phys. Rev. X **6**, 041059 (2016).
[6] D. G. Mazzone, S. Raymond, J. L. Gavilano, E. Ressouche, C. Niedermayer, J. O. Birk, B. Ouladdiaf, G. Bastien, G. Knebel, D. Aoki, G. Lapertot, and M. Kenzelmann, Science Advances **3**, 1602055 (2017).
[7] R. Hu, Y. Lee, J. Hudis, V. F. Mitrovic, and C. Petrovic, Phys. Rev. B **77**, 165129 (2008).
[8] S. Raymond, S. M. Ramos, D. Aoki, G. Knebel, V. P. Mineev, and G. Lapertot, J. Phys. Soc. Jpn. **83**, 13707 (2014), 1307.2592.
[9] C. Stock, C. Broholm, Y. Zhao, F. Demmel, H. J. Kang, K. C. Rule, and C. Petrovic, Phys. Rev. Lett. **109**, 167207 (2012).
[10] S. Raymond and G. Lapertot, Phys. Rev. Lett. **115**, 037001 (2015).
[11] D. G. Mazzone, S. Raymond, J. L. Gavilano, P. Steffens, A. Schneidewind, G. Lapertot, and M. Kenzelmann, Phys. Rev. Lett. **119**, 187002 (2017).
[12] J. H. J. Martiny, M. N. Gastiasoro, I. Vekhter, and B. M. Andersen, Phys. Rev. B **92**, 224510 (2015).
[13] P. F. S. Rosa, J. Kang, Y. Luo, N. Wakeham, E. D. Bauer, F. Ronning, Z. Fisk, R. M. Fernandes, and J. D. Thompson, Proc. Natl. Acad. Sci. **114**, 5384 (2017).

[14] M. A. Tanatar, J. Paglione, S. Nakatsuji, D. G. Hawthorn, E. Boaknin, R. W. Hill, F. Ronning, M. Sutherland, L. Taillefer, C. Petrovic, P. C. Canfield, and Z. Fisk, Phys. Rev. Lett. **95**, 067002 (2005).
[15] J. Paglione, M. A. Tanatar, J.-P. Reid, H. Shakeripour, C. Petrovic, and L. Taillefer, Phys. Rev. Lett. **117**, 016601 (2016).
[16] A. Bianchi, R. Movshovich, N. Oeschler, P. Gegenwart, F. Steglich, J. D. Thompson, P. G. Pagliuso, and J. L. Sarrao, Phys. Rev. Lett. **89**, 137002 (2002).
[17] Y. Tokiwa, R. Movshovich, F. Ronning, E. D. Bauer, P. Papin, A. D. Bianchi, J. F. Rauscher, S. M. Kauzlarich, and Z. Fisk, Phys. Rev. Lett. **101**, 037001 (2008).
[18] Y. Tokiwa, R. Movshovich, F. Ronning, E. D. Bauer, A. D. Bianchi, Z. Fisk, and J. D. Thompson, Phys. Rev. B **82**, 220502 (2010).
[19] K. Izawa, H. Yamaguchi, Y. Matsuda, H. Shishido, R. Settai, and Y. Onuki, Phys. Rev. Lett. **87**, 057002 (2001).
[20] S. Gerber, M. Bartkowiak, J. L. Gavilano, E. Ressouche, N. Egetenmeyer, C. Niedermayer, A. D. Bianchi, R. Movshovich, E. D. Bauer, J. D. Thompson, and M. Kenzelmann, Nat Phys **10**, 126 (2014).
[21] D. G. Mazzone, R. Yadav, M. Bartkowiak, J. L. Gavilano, S. Raymond, E. Ressouche, G. Lapertot, and M. Kenzelmann, Scientific Reports **8**, 1295 (2018).
[22] V. P. Mineev, Low Temperature Physics **43**, 11 (2017).
[23] D. F. Agterberg, M. Sigrist, and H. Tsunetsugu, Phys. Rev. Lett. **102**, 207004 (2009).
[24] S.-Z. Lin and J.-X. Zhu, Phys. Rev. B **96**, 224502 (2017).
[25] P. Fulde and R. A. Ferrell, Phys. Rev. **135**, A550 (1964).
[26] A. I. Larkin and Y. N. Ovchinnikov, Sov. Phys. JETP **20**, 762 (1965).
[27] Y. Hatakeyama and R. Ikeda, Phys. Rev. B **91**, 094504 (2015).
[28] K.-i. Hosoya and R. Ikeda, Phys. Rev. B **95**, 224513 (2017).

[29] D. Y. Kim, S.-Z. Lin, F. Weickert, E. D. Bauer, F. Ronning, J. D. Thompson, and R. Movshovich, Phys. Rev. Lett. **118**, 197001 (2017).

[30] G. Grüner, Rev. Mod. Phys. **66**, 1 (1994).

[31] G. Seyfarth, J. P. Brison, G. Knebel, D. Aoki, G. Lapertot, and J. Flouquet, Phys. Rev. Lett. **101**, 046401 (2008).

[32] M. N. Gastiasoro, F. Bernardini, and B. M. Andersen, Phys. Rev. Lett. **117**, 257002 (2016).